7

Combustion of Energetic Materials

Richard A. Yetter
Penn State University

Princeton-Combustion Institute
2018 Summer School on Combustion
June 25-29, 2018
Princeton, NJ

Additional Reading and References

- Bulusu, S., ed., **Chemistry and Physics of Energetic Materials**, Kluwer Academic Publishers, Boston, 1990.
- Clark, J.D., **Ignition! An Informal History of Liquid Rocket Propella**nts, Rutgers University press, New Brunswick, NJ, 1972.
- Davenas, A., "Development of Modern Solid Propellants," *Journal of Propulsion and Power*, 19 (6), 1108-1128, 2003.
- Dreizin, E.L., "Metal-based Reactive Nanomaterials," *Progress in Energy and Combustion Science*, 35, 141-167, 2009.
- Edwards, T., "Liquid Fuels and Propellants for Aerospace Propulsion 1903-2003," *Journal of Propulsion and Power*, 19 (6), 1089, 2003.
- Glassman, I., Yetter, R.A., and Glumac, N., **Combustion**, 5th Edition, Academic Press, Waltham, MA, 2015
- Jackson, T.L., "Modeling of Heterogeneous Propellant Combustion: A Survey," *AIAA Journal* 50, 5, May 2012, 993
- Kubota, N., **Propellants and Explosives: Thermochemical Aspects of Combustion**, 2nd Edition, Wiley-VCH Verlag GmbH & Co. KGaA, Weinheim, 2007.

Additional Reading and References

- Kuo, K.K. and Summerfield, eds., **Fundamentals of Solid Rocket Propellant Combustion**, American Institute of Aeronautics and Astronautics, Reston, VA, 1984.
- Kuo, K.K., and Acharya, R., **Applications of Turbulent and Multiphase Combustion**, John Wiley and Sons, Hoboken NJ, 2012.
- Sundaram, D., Yang, V., and Yetter, R.A., "Metal-based Nanoenergetic Materials: Synthesis, Properties, and Applications," *Progress in Energy and Combustion Science* 61, 293-365, 2017.
- Sutton, G.P. and Biblarz, O., **Rocket Propulsion Elements: An Introduction to the Engineering of Rockets**, 9th Edition, John Wiley and Sons, New York, 2017.
- Yang, V., Brill, T.B., and Ren, W.-Z., eds., **Solid Propellant Chemistry, Combustion, and Interior Ballistics**, American Institute of Aeronautics and Astronautics, vol. 185, Reston, VA, 2000.
- Yetter, R.A., Risha, G.A., and Son, S.F., "Metal Particle Combustion and Nanotechnology," *Proceedings of the Combustion Institute* 32, 1819-1838, 2009.

Appendixes

Constant Volume Temporal Reacting System

$$\frac{dY_j}{dt} = \upsilon \dot{\omega}_j MW_j \quad (j = 1, ..., \mathrm{K})$$

$$C_v \frac{dT}{dt} = -\upsilon \sum_{j=1}^{K} e_j \dot{\omega}_j MW_j$$

$$\upsilon = V / m$$

$$\sum_{j=1}^{n} \nu'_{ji} \mathrm{M}_j \leftrightarrow \sum_{j=1}^{n} \nu''_{ji} \mathrm{M}_j \quad i, = 1, ..., m$$

$$q_i = k_{f,i} \prod_{j=1}^{n} \left(\mathrm{M}_j\right)^{\nu'_{ji}} - k_{b,i} \prod_{j=1}^{n} \left(\mathrm{M}_j\right)^{\nu''_{ji}}$$

$$\dot{\omega}_{ji} = \left[\nu''_{ji} - \nu'_{ji}\right] q_i = \nu_{ji} q_i$$

$$\dot{\omega}_j = \sum_{i=1}^{m} \nu_{ji} q_i$$

T: temperature
Y_k: mass fraction of j^{th} species
MW_k: molecular weight of j^{th} species
t: time
υ: specific volume
V: volume of system
m: mass of system
e_k: internal energy of j^{th} species
C_v: constant volume heat capacity
$\dot{\omega}_j$: molar rate of production of j^{th} species
M: species
k_f, k_b: forward and backward rate constants for the i_{th} reaction
ν: stoichiometric coefficients for the i^{th} reaction and j^{th} species of the reactants or products

Model for RDX Combustion by Liau and Yang

Model for RDX Combustion by Liau and Yang - The Gas-Phase

- The gas-phase continuity equation

$$\frac{\partial \rho}{\partial t}+\frac{\partial}{\partial x}(\rho u)=0$$

- The gas-phase species conservation equations are:

$$\frac{\partial(\rho Y_i)}{\partial t}+\frac{\partial}{\partial x}\left[\rho Y_i\left(u+V_i\right)\right]=\dot{\omega}_i \quad (i=1,2,\ldots N)$$

- The gas-phase energy conservation equation

$$\frac{\partial(\rho e)}{\partial t}+\frac{\partial(\rho u e)}{\partial x}=\frac{\partial}{\partial x}\left(\lambda\frac{\partial T}{\partial x}-\sum_{k=1}^{N}\rho Y_k V_k h_k\right)-p\frac{\partial u}{\partial x}$$

- The gas-phase enthalpy of the kth species

$$h_k=\left[\int_{T_{ref}}^{T} C_{p,k}\,dT+h_{s,k}\left(T_{ref}\right)\right]+\Delta h^0_{f,k}$$

- The diffusion velocity is evaluated as

$$V_k=-\frac{D_k}{X_k}\frac{\partial X_k}{\partial x};\;\; D_k=\frac{1-Y_k}{\sum_{j\neq k} X_j/D_{jk}}$$

Model for RDX Combustion by Liau and Yang - The Gas-Phase

- The equation of state for a multicomponent system

$$p = \rho R_u T \sum_{k=1}^{N} \frac{Y_k}{MW_k}$$

- The general chemical reaction is represented as

$$\sum_{i=1}^{N} \nu_i^{'} M_i \underset{k_{bj}}{\overset{k_{fj}}{\rightleftarrows}} \sum_{i=1}^{N} \nu_i^{''} M_i$$

- The reaction rate constant for the *jth* forward and backward reactions are expressed in Arrhenius form

$$k_j = A_j T^b \, exp\left(-\frac{E_{a_j}}{R_u T} \right)$$

- The rate of change of molar species *i* by the *jth* reaction is

$$\dot{C}_{M_{ij}} = \left(\nu_{ij}'' - \nu_{ij}' \right) \left[k_{f,j} \prod_{i=1}^{n} \left(C_{M_i} \right)^{\nu_{ij}'} - k_{b,j} \prod_{i=1}^{n} \left(C_{M_i} \right)^{\nu_{ij}''} \right]$$

- The total rate of change of species *i* is

$$\dot{\omega}_i = MW_i \sum_{j=1}^{N_R} \dot{C}_{M_{ij}}$$

Model for RDX Combustion by Liau and Yang- The Foam Layer Region

- A two phase fluid dynamic model using a spatial averaging technique was employed to formulate the physicochemical processes in the foam layer region
- These processes include thermal decomposition, evaporation, bubble formation, gas-phase reactions in bubbles, and interfacial transport of mass and energy between gas and condensed phases
- The formulation is based on the control volume approach for conservation equations with the control volumes for gas bubbles and condensed phases complementary to each other
- The Dupuit-Forchheimer assumption is used that allows the fractional-volume void fraction (or porosity) to be extended to a fractional area void fraction definition

  $$A_g = \phi A$$

  where ϕ is the void fraction, A_g is the fractional cross-sectional area consisting of gas bubbles in foam layer, and A is the cross-sectional area of the propellant

Model for RDX Combustion by Liau and Yang- The Foam Layer Region

- The gas-phase mass conservation equation

$$\frac{\partial \phi \rho_g}{\partial t} + \frac{\partial}{\partial x}\left(\phi \rho_g u_g\right) = \dot{\omega}_{c \to g}$$

- The gas-phase species conservation equations are:

$$\frac{\partial\left(\phi \rho_g Y_{gi}\right)}{\partial t} + \frac{\partial}{\partial x}\left[\phi \rho_g Y_{gi}\left(u_g + V_{gi}\right)\right] = \dot{\omega}_{gi} \quad \left(i = 1,2,\ldots N_g\right)$$

- The gas-phase energy conservation equation

$$\frac{\partial\left(\phi \rho_g e_g\right)}{\partial t} + \frac{\partial\left(\phi \rho_g u_g e_g\right)}{\partial x} = \frac{\partial}{\partial x}\left(\phi \lambda_g \frac{\partial T_g}{\partial x} - \phi \sum_{k=1}^{N_g} \rho_g Y_{gk} V_{gk} h_{gk}\right) - p\phi \frac{\partial u_g}{\partial x} + \dot{\omega}_{c \to g} q_{c \to g} + A_s h_c \left(T_c - T_g\right)$$

where $q_{c \to g}$ is the heat evolved during pyrolysis of condensed-phase to gas-phase, $\dot{\omega}_{c \to g}$ is the rate of conversion of condensed phase material to gas-phase products, A_s is the interface area between bubbles and liquid per unit volume, and h_c is the heat transfer coefficient

Model for RDX Combustion by Liau and Yang- The Foam Layer Region

- The condensed-phase mass conservation equation

$$\frac{\partial (1-\phi)\rho_c}{\partial t} + \frac{\partial}{\partial x}\left((1-\phi)\rho_c u_c\right) = -\dot{\omega}_{c\to g}$$

- The condensed-phase species conservation equations

$$\frac{\partial\left((1-\phi)\rho_c Y_{ci}\right)}{\partial t} + \frac{\partial}{\partial x}\left[(1-\phi)\rho_c Y_{ci}\left(u_c + V_{ci}\right)\right] = \dot{\omega}_{ci} \quad \left(i = 1,2,\ldots N_c\right)$$

- The condensed-phase energy conservation equation

$$\frac{\partial\left((1-\phi)\rho_c e_c\right)}{\partial t} + \frac{\partial\left((1-\phi)\rho_c u_c e_c\right)}{\partial x} = \frac{\partial}{\partial x}\left((1-\phi)\lambda_c \frac{\partial T_c}{\partial x} - (1-\phi)\sum_{k=1}^{N_c}\rho_c Y_{ck} V_{ck} h_{ck}\right) - p(1-\phi)\frac{\partial u_c}{\partial x} - \dot{\omega}_{c\to g} q_{c\to g} - A_s h_c\left(T_c - T_g\right)$$

Model for RDX Combustion by Liau and Yang-Reactions in The Foam Layer Region

- $RDX_{(l)} \rightarrow 3CH_2O + 3N_2O$

$$\dot{\omega}_1 = (1-\phi)\rho_c k_1, \quad k_1(1/s) = 6\times10^{13}\, exp\left[-36.0(kcal/mol)/R_u T\right]$$

- $RDX_{(l)} \rightarrow 3HCN + 1.5NO_2 + 1.5NO + 1.5H_2O$

$$\dot{\omega}_2 = (1-\phi)\rho_c k_2, \quad k_2(1/s) = 16\times10^{16}\, exp\left[-45.0(kcal/mol)/R_u T\right]$$

- A secondary reaction was also considered

$NO_2 + CH_2O \rightarrow NO + CO + H_2O$

$$\dot{\omega}_3 = \phi k_3 \frac{\rho_g Y_{CH_2O}}{MW_{CH_2O}} \frac{\rho_g Y_{NO_2}}{MW_{NO_2}},$$

$$k_3\left(cm^3/mol-s\right) = 802\times T^{2.77}\, exp\left[-13.73(kcal/mol)/R_u T\right]$$

- In addition to thermal decomposition, the thermodynamic phase transition from liquid to vapor RDX is considered

$RDX_{(c)} \leftrightarrow RDX_{(g)}$

Model for RDX Combustion by Liau and Yang-Evaporation and Condensation Considerations of RDX

- The condensation flux can be characterized in terms of the rate at which vapor molecules collide and stick to the interface

$$\dot{m}''_{condensation} = s\dot{n}''MW = s\left(\frac{1}{4}\sqrt{\frac{8R_uT}{\pi MW}}\right)\left(\frac{p}{RT}\right)X^{0^+}$$

- If thermodynamic phase equilibrium is achieved, evaporation proceeds at the same rate as condensation

$$\dot{m}''_{evap} = \dot{m}''_{condensation} = s\dot{n}''MW = s\left(\frac{1}{4}\sqrt{\frac{8R_uT}{\pi MW}}\right)\left(\frac{p}{RT}\right)\left(\frac{p_{v,eq}}{p}\right)$$

- The vapor pressure can be approximated by the Clausius Clapeyron equation

$$p_{v,eq} = p_0\, exp\left[-\Delta H_{vap} / \left(R_uT\right)\right]$$

- At nonequilibrium conditions, the net evaporation rate is

$$\dot{m}''_{net} = \dot{m}''_{evap} - \dot{m}''_{condensation}$$

Model for RDX Combustion by Liau and Yang-Evaporation and Condensation Considerations of RDX

- Thus, the specific mass conversion rate due to evaporation is

$$\dot{\omega}_{c \rightleftarrows g} = A_s \dot{m}''_{net}$$

- The specific surface area is a function of the void fraction and number density of bubbles

$$A_s = \left(36\pi n_b\right)^{1/3} \phi^{2/3} \qquad \phi < 1/2$$

$$A_s = \left(36\pi n_b\right)^{1/3} \left(1-\phi\right)^{2/3} \qquad \phi \geq 1/2$$

where n_b is the number density of bubbles determined empirically

Model for RDX Combustion by Liau and Yang- Boundary Conditions

- With application of conservation laws to the propellant surface, the matching conditions at the gas-foam layer interface are:
- Mass Flux:

$$\left[(1-\phi)\rho_c u_c + \phi\rho_g u_g\right]_{0^-} = (\rho u)_{0^+}$$

- Species Flux:

$$\left[(1-\phi)\rho_c\left(u_c + V_{c_i}\right)Y_{c_i} + \phi\rho_g\left(u_g + V_{g_i}\right)Y_{g_i}\right]_{0^-} = \left(\rho\left(u + V_i\right)Y_i\right)_{0^+}$$

- Energy Flux:

$$\left[(1-\phi)\lambda_c\frac{dT_c}{dx} - \sum_{i=1}^{N_c}(1-\phi)\rho_c\left(u_c + V_{c_i}\right)Y_{c_i}h_{c_i}\right]_{0^-} + \left[\phi\lambda_g\frac{dT_g}{dx} - \sum_{i=1}^{N_g}\phi\rho_g\left(u_g + V_{g_i}\right)Y_{g_i}h_{g_i}\right]_{0^-}$$

$$= \left[\lambda\frac{dT}{dx} - \sum_{i=1}^{N}\rho\left(u + V_i\right)Y_i h_i\right]_{0^+}$$

- Phase transition from liquid to vapor RDX at the interface:

$$\left[(1-\phi)\rho_c u_c\right]_{0^-} = \dot{m}''_{net}$$

Model for RDX Combustion by Liau and Yang-Boundary Conditions

- In the foam layer, it is assumed $T_c = T_g$
- The far field conditions for the gas phase require that the gradients of the flow properties be zero as $x \rightarrow \infty$

$$\frac{\partial \rho}{\partial x} = \frac{\partial u}{\partial x} = \frac{\partial T}{\partial x} = \frac{\partial Y_i}{\partial x} = 0$$

- The conditions at the cold boundary for the condensed phase ($x \rightarrow -\infty$) are

$T_c = T_i$ and $\phi = 0$ at $x \rightarrow \infty$

Application of Energetic Materials to Rocket Propulsion

Solid Propellants Used in Rockets

- A major application of solid propellants is in rockets
- Burning solid propellants produces high-temperature combustion products, which can be expanded through a converging-diverging nozzle to generate thrust for rocket propulsion
- Generally, there are two types of solid propellant grains that are used in rockets
  - Side burning type:

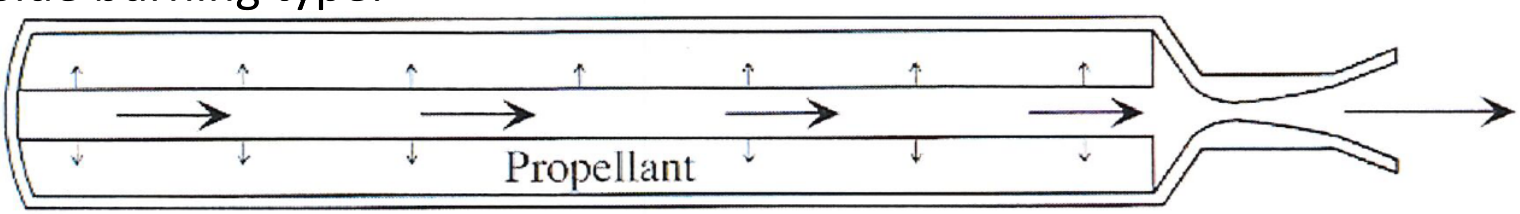

Side Burning Type of Solid Propellant Rocket Motor

  - End burning type:

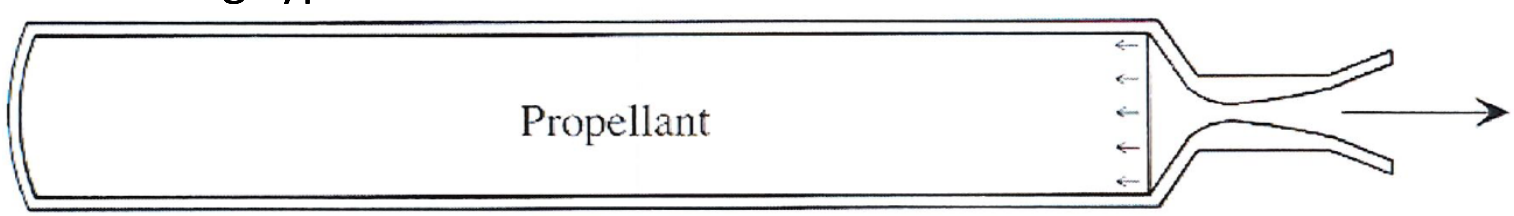

End Burning Type of Solid Propellant Rocket Motor

From Kubota, 2007

Thrust of a Solid Rocket Motor

- Thrust is a result of pressure force distribution over interior and exterior surfaces of the motor
- It can be expressed in an equation as follow:

$$F = \oint P dA = \dot{m}_p V_e + A_e \left(P_e - P_{amb} \right) \qquad (36)$$

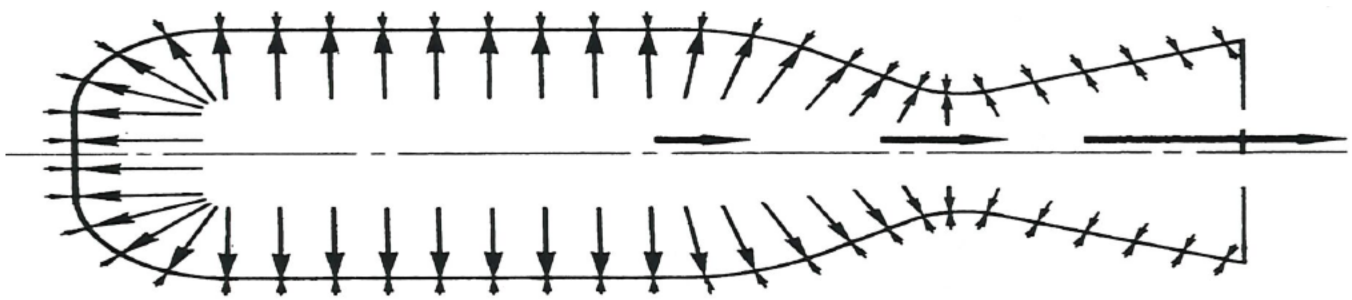

- The thrust is also expressed in terms of a dimensionless thrust coefficient C_F, the nozzle throat area A_t, and the average chamber pressure P_c

$$F = C_F A_t P_c \qquad (37)$$

Thrust of a Solid Rocket Motor (cont.)

Nozzle exit has a divergence angle α_d, which implies that not all the jet momentum ($\dot{m}_p V_e$) is in the axial direction. Therefore, a λ parameter is introduced to account for loss of axial momentum in the thrust calculations.

This parameter λ can be evaluated from:

$$\lambda = \frac{1+\cos\alpha_d}{2} \qquad (38)$$

With this correction, the thrust of a rocket motor can be evaluated from

$$F = \lambda \dot{m}_p V_e + A_e \left(p_e - p_{amb} \right) \qquad (39)$$

From the isentropic flow relationships, the nozzle exit flow velocity is determined from:

$$V_e = \sqrt{\frac{2\gamma}{\gamma-1} R T_c \left[1 - \left(\frac{p_e}{p_c} \right)^{\frac{\gamma-1}{\gamma}} \right]} \qquad (40)$$

Thrust of a Solid Rocket Motor (cont.)

The mass generation rate of a non-metallized solid propellant must be equal to the mass flow rate through a choked nozzle under *steady-state operation*. Then, using the choked flow equation, $\dot{m}_g$ can be related to the chamber pressure P_c and temperature T_c as:

$$\dot{m}_p = \dot{m}_g = \dot{m}_d = \Gamma(\gamma)\frac{p_c A_t}{\sqrt{RT_c}} \tag{41}$$

where Γ is defined as:

$$\Gamma(\gamma) = \sqrt{\gamma}\left(\frac{2}{\gamma+1}\right)^{\frac{\gamma+1}{2(\gamma-1)}} \tag{42}$$

Using Eqs. (38), (40) and (41) into Eq. (30), we have the following expression for the thrust:

$$F = p_c A_t\left\{\lambda\Gamma\sqrt{\frac{2\gamma}{\gamma-1}\left[1-\left(\frac{p_e}{p_c}\right)^{\frac{\gamma+1}{2(\gamma-1)}}\right]}+\frac{A_e}{A_t}\left(\frac{p_e}{p_c}-\frac{p_{amb}}{p_c}\right)\right\} \tag{43}$$

Thrust of a Solid Rocket Motor (cont.)

A comparison of Eq. (37) with Eq. (41) yields the following expression for the thrust coefficient C_F:

$$C_F = \left\{ \lambda \Gamma \sqrt{\frac{2\gamma}{\gamma - 1}\left[1 - \left(\frac{p_e}{p_c}\right)^{\frac{\gamma+1}{2(\gamma-1)}}\right]} + \frac{A_e}{A_t}\left(\frac{p_e}{p_c} - \frac{p_{amb}}{p_c}\right)\right\} = \lambda C_{F0} + \frac{A_e}{A_t}\left(\frac{p_e}{p_c} - \frac{p_{amb}}{p_c}\right) \quad (44)$$

The mass balance in the rocket motor can be written as:

$$\frac{dm_{CV}}{dt} = \frac{d\left(\rho_g V_{CV}\right)}{dt} = \dot{m}_g - \dot{m}_d \quad (45)$$

The rate of mass generation by solid-propellant burning for a non-metallized propellant is:

$$\dot{m}_g = \dot{m}_p = \rho_p A_b r_b \quad (46)$$

The rate of mass discharge through the nozzle is:

$$\dot{m}_d = C_D A_t p_c \quad (47)$$

Total Impulse of a Solid Rocket Motor

The mass flow factor C_D in Eq. (47) is:

$$C_D \equiv \frac{\Gamma(\gamma)}{\sqrt{RT_c}} = \sqrt{\gamma\left(\frac{2}{\gamma+1}\right)^{\frac{\gamma+1}{\gamma-1}} \frac{MW}{R_u T_c}} \quad \text{Dimensions of } C_D \left[\frac{time}{length}\right] \tag{48}$$

Note that the parameter C_D should not be confused with the dimensionless discharge coefficient C_d

For steady-state burning conditions, the mass balance equation Eq. (45) can be written as: $\dot{m}_g = \dot{m}_d$ By utilizing Eq. (37), we have:

$$\rho_p A_b r_b = C_D A_t p_c = \frac{C_D}{C_F} F \tag{49}$$

Total impulse is the thrust force integrated over burning time:

$$I_t = \int_0^t F dt \quad \text{Units: (N-s)} \tag{50}$$

Specific Impulse of a Solid Rocket Motor

The specific impulse is defined as the total impulse per unit weight of propellant burnt:

$$I_{sp} \equiv \frac{\int_0^t F dt}{g_0 \int_0^t \dot{m}_g dt} = \frac{I_t}{g_0 m_p} = \frac{I_t}{W_p} \quad \text{Units: (s)} \tag{51}$$

where g_0 (=9.8066 m/s^2 or 32.175 ft/s^2) is the gravitational acceleration at sea level

Other Performance Parameters

- If we consider constant thrust level for the majority of motor operation time as shown in the following figure

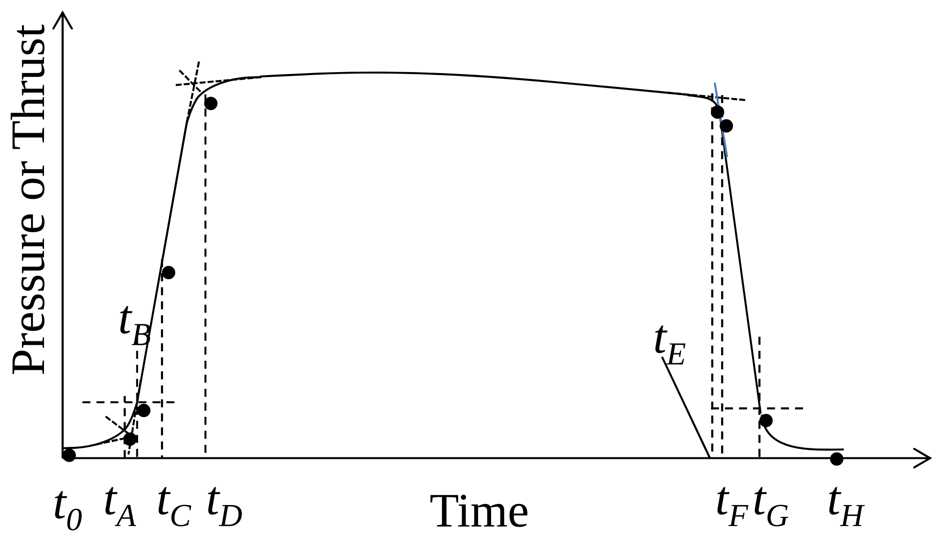

t_0: Initiation time
t_A: Start of thrust rise due to igniter
t_B: Start of the propellant burning
t_C: Time when pressure or thrust is equal to half of the steady-state value
t_D: End of chamber volume filling period
t_E: End of the propellant burning
t_F: Point of maximum rate of change of curvature during tail-off period
t_G: Fixed percentage of p_{avg} or p_{max}
t_H: End of motor thrust

- In the above case of static firing of the solid rocket motor, the average thrust can be defined as:

$$F_{avg} = \frac{1}{t_E - t_C} \int_{t_C}^{t_E} F dt \tag{52}$$

- Similarly, the average pressure is defined as:

$$p_{avg} = \frac{1}{t_E - t_C} \int_{t_C}^{t_E} p dt \tag{53}$$

Other Performance Parameters of Solid Rocket Motors

In case of constant thrust operation, the specific impulse is:

$$I_{sp} \cong \frac{F}{\dot{m}_p g_0} \tag{54}$$

From Eq. (49), the thrust can be written as:

$$F = \frac{C_F}{C_D} \dot{m}_p \tag{55}$$

Substituting Eq. (55) in Eq. (54), we have:

$$I_{sp} = \frac{C_F}{C_D g_0} \tag{56}$$

Substituting C_D in the above equation, we have:

$$I_{sp} = \frac{C_F}{g_0 \sqrt{\gamma \left(\frac{2}{\gamma + 1} \right)^{\frac{\gamma+1}{\gamma-1}} \frac{1}{R_u}}} \sqrt{\frac{T_c}{MW}} \text{ or } I_{sp} \propto \sqrt{\frac{T_c}{MW}} \tag{57}$$

Propellants with high T_f and low MW products are desirable

Variation of Thrust Coefficient with Area Expansion Ratio

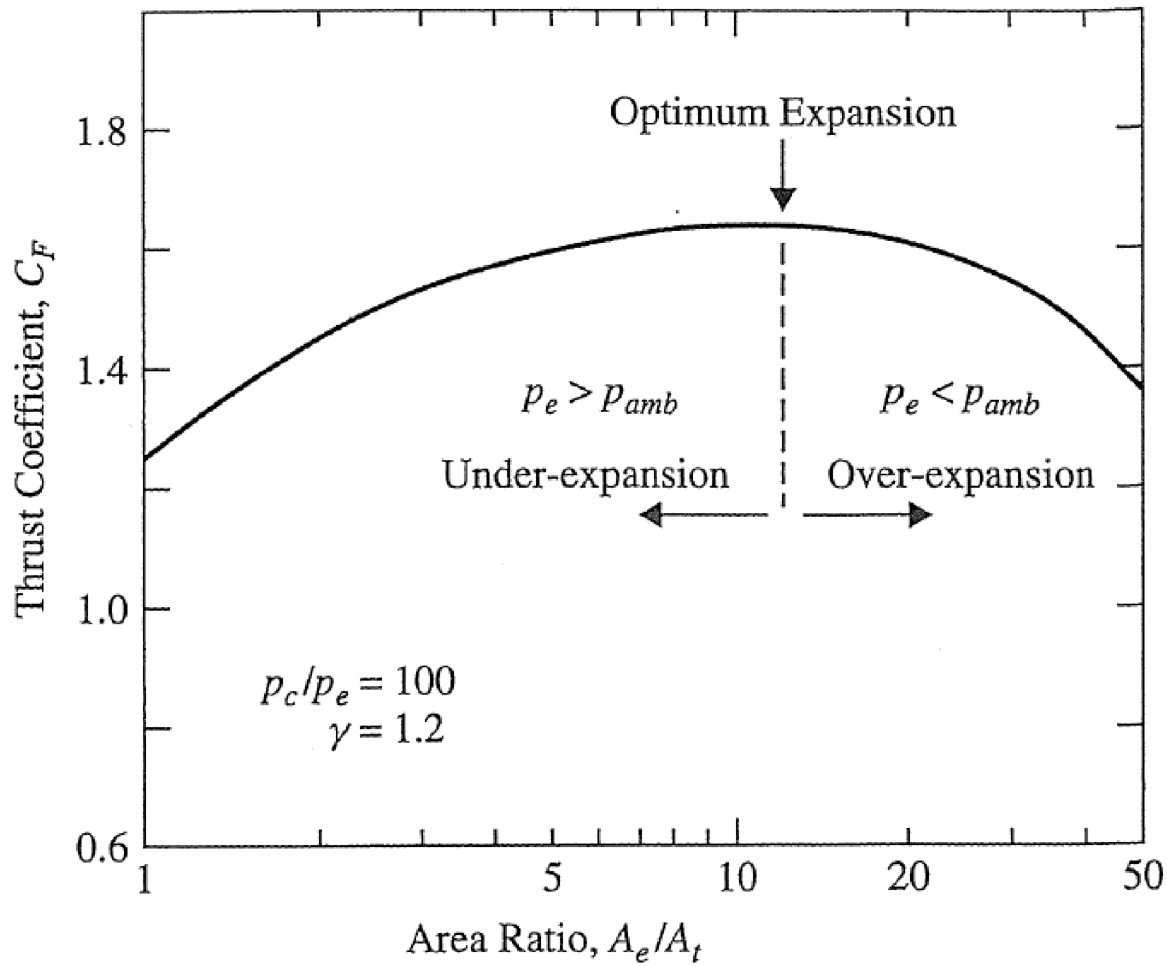

- For maximum C_F, it is desirable to have combustion products expanded to the ambient pressure.
- At optimum expansion , $P_e = P_{amb}$

From Kuo and Acharya, 2012

Variation of Thrust Coefficient with Area Expansion Ratio at Several Specified Pressure Ratios

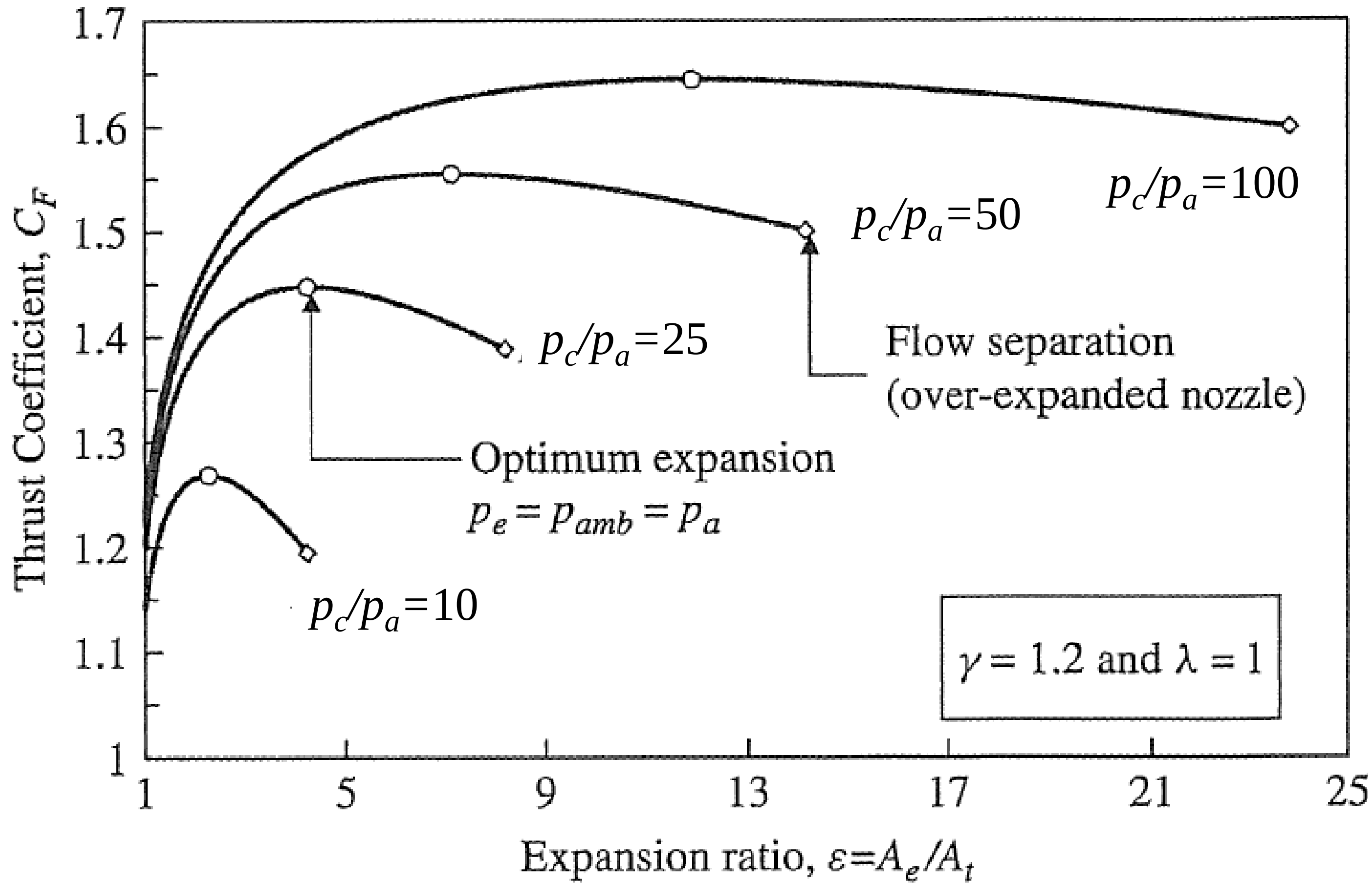

- The maximum on each curve represents the optimum expansion condition
- Note that during a flight of a rocket, optimum expansion is achieved only at one altitude

From Kuo and Acharya, 2012

Dependency of I_{sp} on T_c/MW

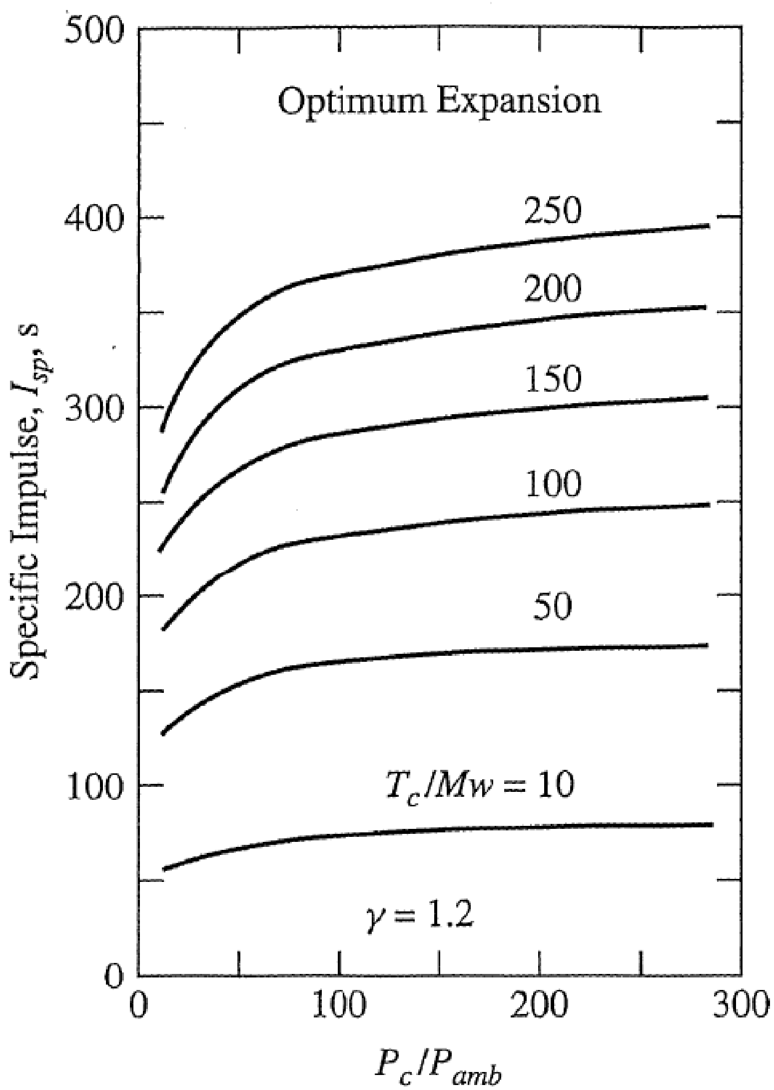

$$I_{sp} \propto \sqrt{\frac{T_c}{MW}}$$

- Under optimum expansion, i.e., $P_e = P_{amb}$
- The effect of P_c/P_e can also be observed from this plot
- It can be seen that T_c/MW has a much stronger effect on I_{sp}

Note $MW = Mw$

From Kuo and Acharya, 2012b

Variation of Flame Temperature and Specific Impulse with NG Concentration of a Double-Base Propellant

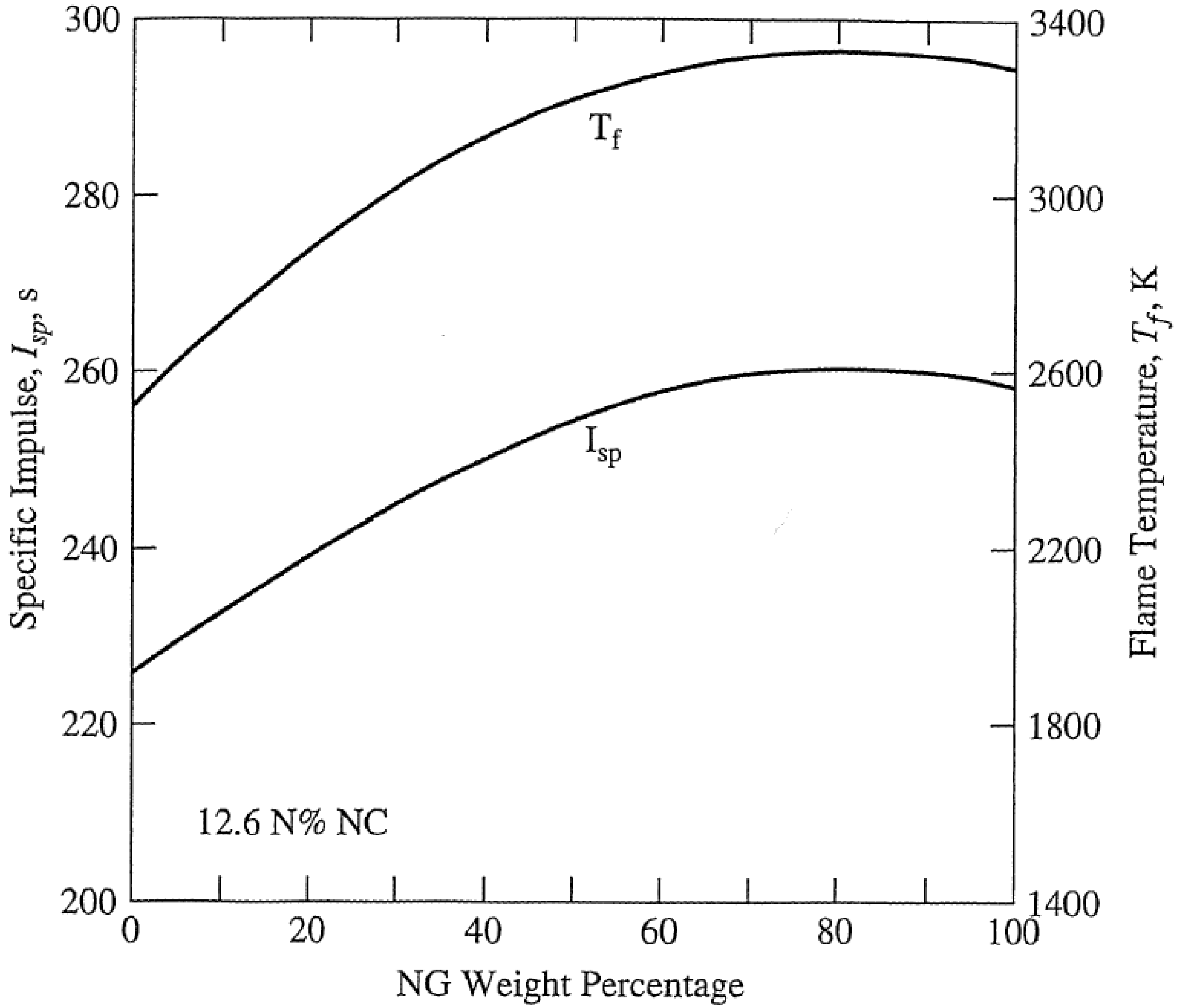

From Kuo and Acharya, 2012

Variation of I_{sp} and T_f with AP or RDX Weight Percentage of CMDB Propellants

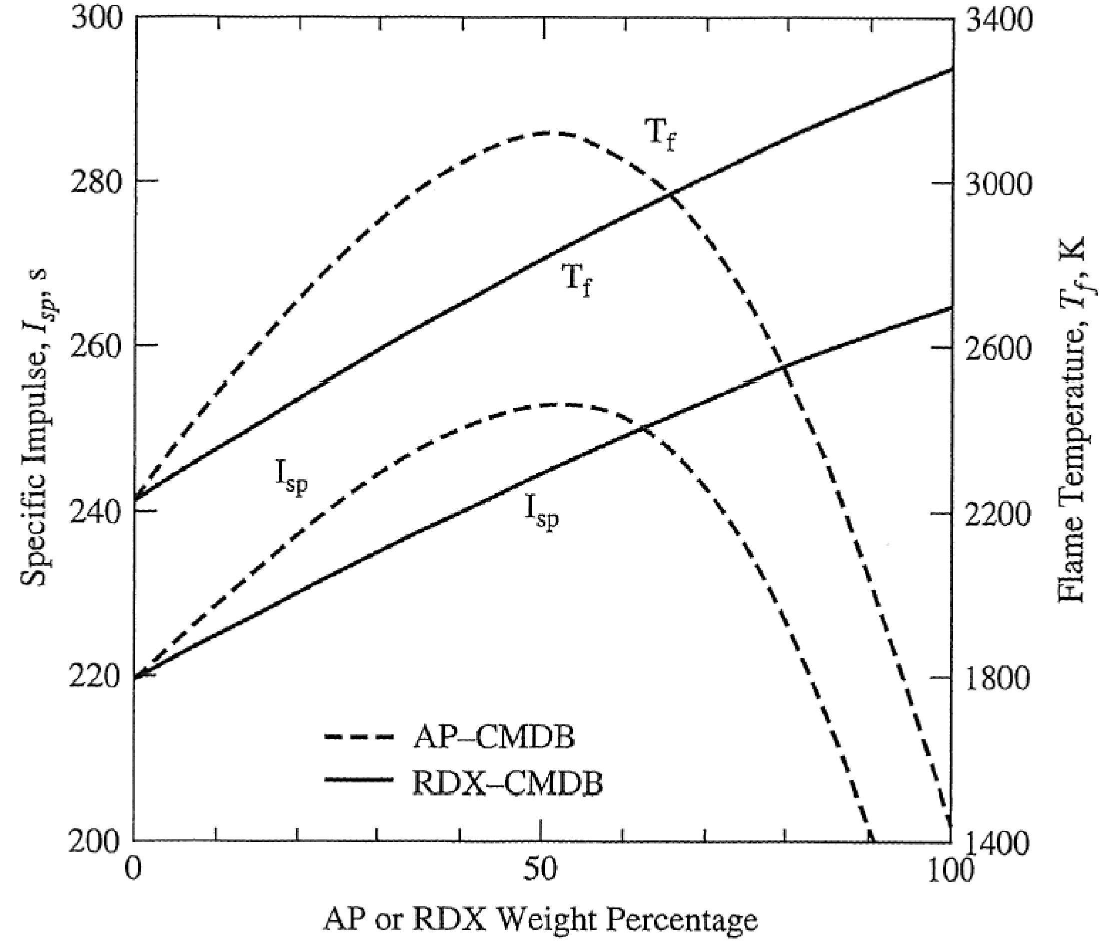

- CMBD = composite modified double base propellant
- At very high RDX wt %, the material properties are poor; hence they cannot be used as true propellants
- Solids loadings above ~ 88 wt % not practical

From Kuo and Acharya, 2012

Density I_{sp}

- For some rockets, performance is measured by the "density-I_{sp}", which is defined as the product of propellant density and specific impulse; i.e.,

$$DI_{sp} \equiv \rho I_{sp} = \rho_p \times I_{sp} \qquad (58)$$

- In order to accommodate a large weight of propellant in a given vehicle tank space, a dense propellant is preferred. This permits smaller vehicle size and weight, which also results in lower aerodynamic drag.
- The average propellant density has an important effect on the maximum flight velocity and range of any rocket-powered vehicle
- The average propellant density can be increased by adding heavy materials such as aluminum powders into the propellant mixture

Characteristic Velocity C^*

A characteristic velocity C^* is defined as a measure of energy available to generate thrust after combustion of the propellant. It is defined as:

$$C^* = \frac{\int_{t_0}^{t_E} p_c A_t \, dt}{m_p} \qquad (59)$$

If the chamber pressure is constant for major part of the rocket operation, then C^* can be written as:

$$C^* = \frac{p_c A_t}{\dot{m}_p} = \frac{\sqrt{R_u}}{\Gamma}\sqrt{\frac{T_c}{MW}} = \frac{1}{C_D} \qquad (60)$$

C^* is a fundamental performance parameter, similar to the I_{sp}. Both of these parameters depend on $\sqrt{T_c / MW}$ by a linear relationship.

Typical values for C^* range from 800 to 1,800 m/s. Higher values correspond to more energetic propellants, which can produce greater thrust and impulse. Using the definition of C^*, thrust can be expressed as:

$$F = \dot{m}_p C_F C^* \qquad (61)$$

Characteristic Velocity, C^*, for a non-Metallized Composite Propellant

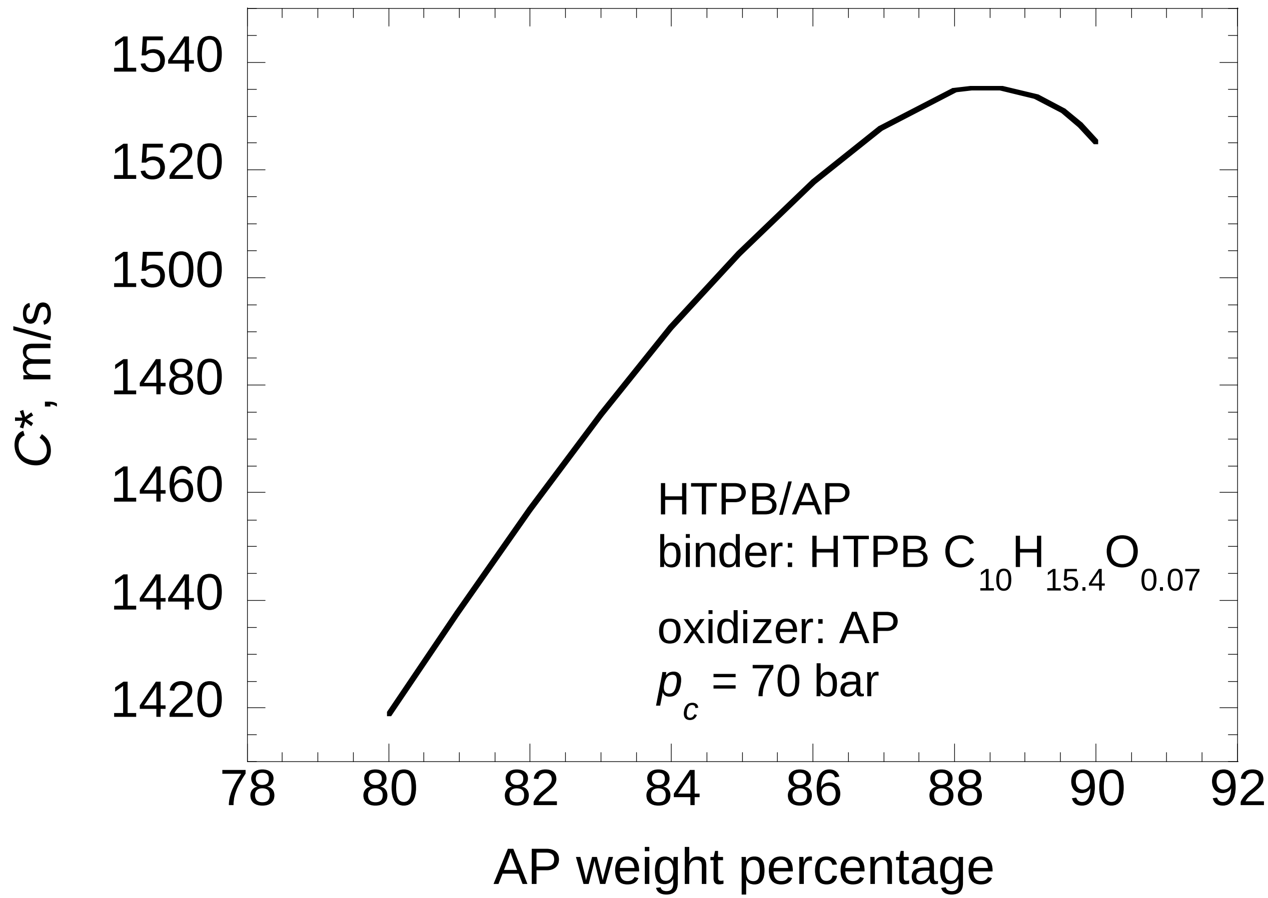

- C^* is a function of propellant formulation as shown above
- The solids loading should be approximately 88% for maximum performance

From Kuo and Acharya, 2012

Characteristic Velocity, C^*, for a Metallized Composite Propellant

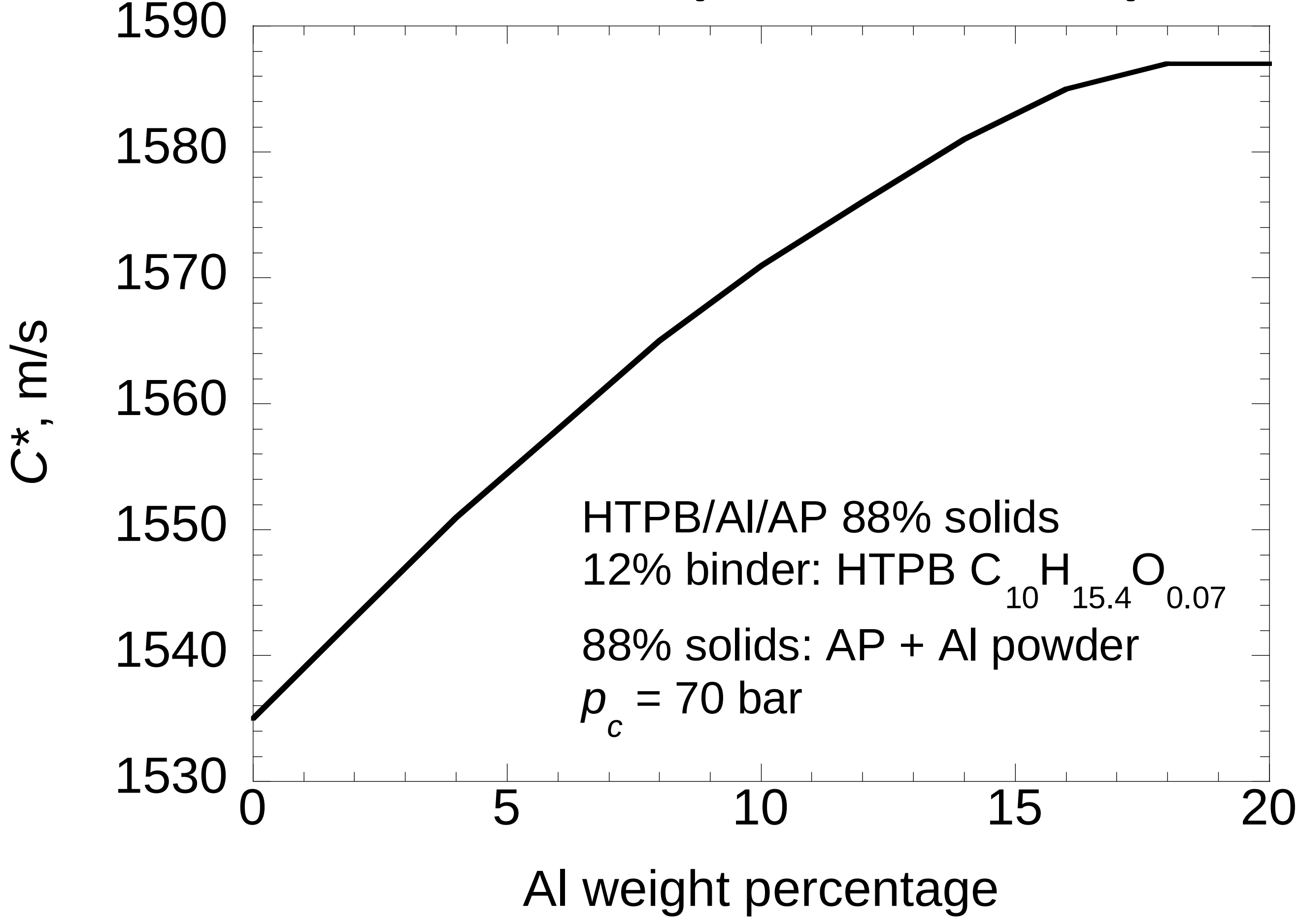

- Note the upper limit for Al powder is near 18% by weight for maximum performance

From Kuo and Acharya, 2012

Effect of Pressure Exponent on Stability of a Solid Rocket Motor

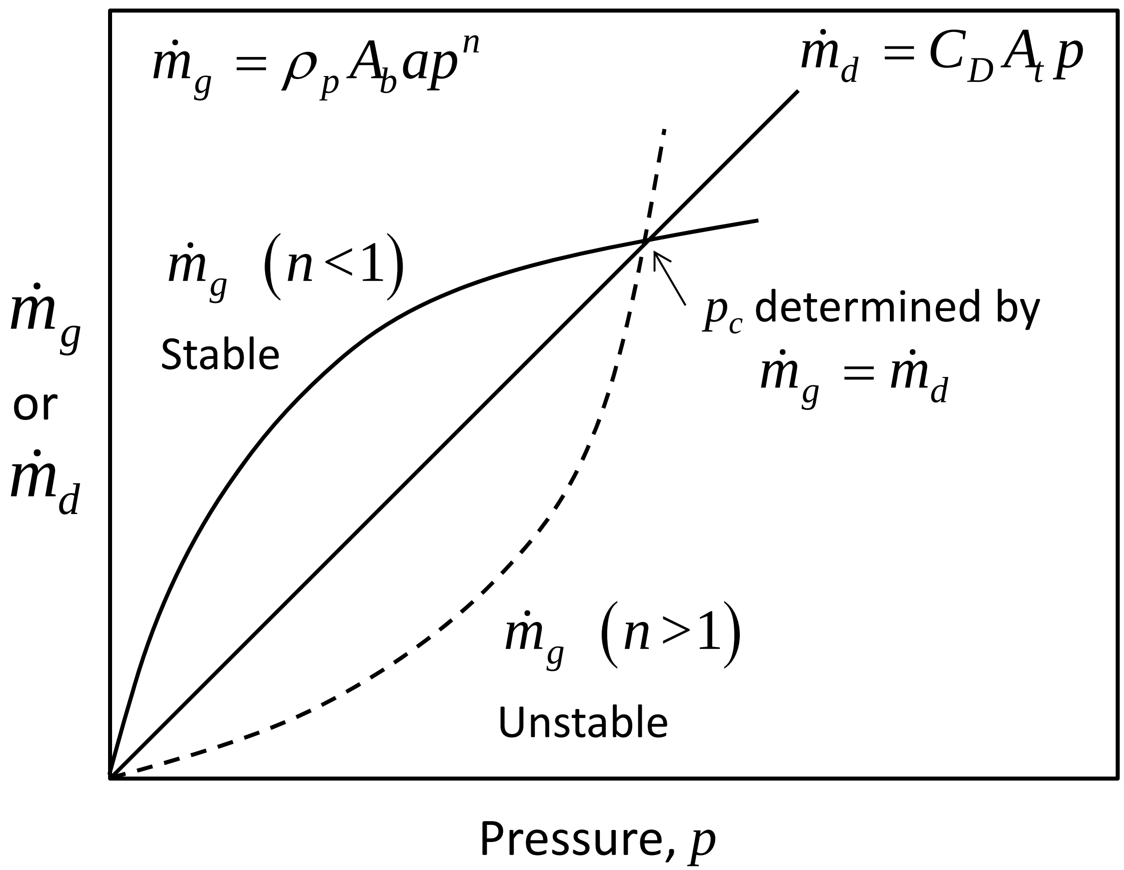

After Kubota, 2001

- Mass discharge rate from rocket motor is proportional to pressure, i.e.,

$$\dot{m}_d \propto P_c$$

- The mass generation rate from propellant is proportional to P^n, i.e.,

$$\dot{m}_g \propto P_c^n$$

- If $n > 1$, any pressure fluctuation in the motor will lead to either overpressure or a dramatic decrease in chamber pressure resulting in extinction of the solid propellant combustion process
- Thus, solid propellants for rocket motors should have $n < 1$

Pressure Sensitivity of Burning Rate

The parameter K_n is defined as the ratio of burning surface area of the solid propellant to the nozzle throat area of a rocket motor; i.e.,

$$K_n \equiv A_b / A_t \tag{62}$$

The pressure sensitivity π_k of the rocket motor combustor is defined as:

$$\pi_k \equiv \frac{1}{p}\left[\frac{\partial p}{\partial T_i}\right]_{K_n} \tag{63}$$

The pressure in the solid-propellant rocket motor combustion chamber can be expressed:

$$p = p_{ref}\, exp\left(\pi_k \left(T_i - T_{i,ref}\right)\right) \tag{64}$$

Therefore, the pressure sensitivity of a rocket motor can be written as:

$$\pi_k = \frac{ln\left(p / p_{ref}\right)}{\left(T_i - T_{i,ref}\right)} \tag{65}$$

The relationship between σ_p and π_k is given by the following equation with pressure exponent n treated as a constant:

$$\sigma_p = \left(1 - n\right)\pi_k \tag{66}$$

Thrust Coefficient, C_F – Efficiency, η

The thrust coefficient for a period of operation is defined as:

$$C_{F,ex} = \frac{\int_{t_0}^{t_E} F(t)\,dt}{\int_{t_0}^{t_E} A_t(t)\,p_c(t)\,dt} \tag{67}$$

Recall that the theoretical thrust coefficient $C_{F,th}$ based upon Eq. (44) can be written as:

$$C_{F,th} = \lambda C_{F0} + \frac{A_e}{A_t}\left(\frac{p_{e,avg}}{p_{c,avg}} - \frac{p_{amb}}{p_{c,avg}}\right) \tag{68}$$

In the theoretical calculations of $C_{F,th}$, no erosion of the nozzle throat is assumed. For experimental test conditions, the nozzle throat size could increase due to thermo-chemical erosion. The experimental value of C_F, can be evaluated from Eq. (67). The average thrust-coefficient efficiency or thrust efficiency is then defined as:

$$\eta \equiv \frac{C_{F,experimental}}{C_{F,theoretical}} = \frac{C_{F,ex}}{C_{F,th}} \tag{69}$$

Properties and Performance Parameters of Different Oxidizers at p = 70 atm

Oxidizer	Chemical Formula	State	ρ (g/cm^3)	$\Delta H_f(298)$ (cal/mol)	T_c (K)	MW (g/mol)	I_{sp} (s)
NC(12.6%N)	$C_6H_{7.55}O_{5(}NO_2)_{2.45}$	S	1.66	-160.2	2586	24.7	230
NC(14.14%)	$C_6H_{7.0006}N_{2.9994}O_{10.9987}$	S	1.66	-155.99	3025	26.8	243
NG	$C_3H_5O_3(NO_2)_3$	L	1.60	-9.75	3289	28.9	244
TMETN	$C_5H_9O_3(NO_2)_3$	L	1.47	-97.8	2898	23.1	253
TEGDN	$C_6H_{12}O_4(NO_2)_2$	L	1.33	-181.6	1376	19.0	183
DEGDN	$C_4H_8O_3(NO_2)_2$	L	1.39	-103.5	2513	21.8	241
ADN	$H_4N_4O_4$	S	1.82-1.84	-36.01	2051	24.8	202
AN	NH_4NO_3	S	1.73	-87.37	1247	22.9	161
AP	NH_4ClO_4	S	1.95	-70.73	1406	27.9	157
HNF	$CH_5H_5O_6$	S	1.87-1.93	-17.22	3082	26.4	254
HNIW(CL-20)	$C_6H_6N_{12}O_{12}$	S	2.04	99.35	3591	27.4	273
NP	NO_2ClO_4	S	2.22	8.88	597	36.4	85
RDX	$C_3H_6N_3(NO_2)_3$	S	1.82	14.69	3286	24.3	266
HMX	$C_4H_8N_4(NO_2)_4$	S	1.90	17.92	3278	24.3	266
TAGN	$CH_9H_7O_3$	S	1.59	-11.5	2050	18.6	231

HNIW: Hexanitrohexaazaisowurtzitane

TAGN: Triaminoguanidinim Nitrate

Variation of MW and T_f of Several HTPB-based Solid Propellants with Oxidizer Concentration

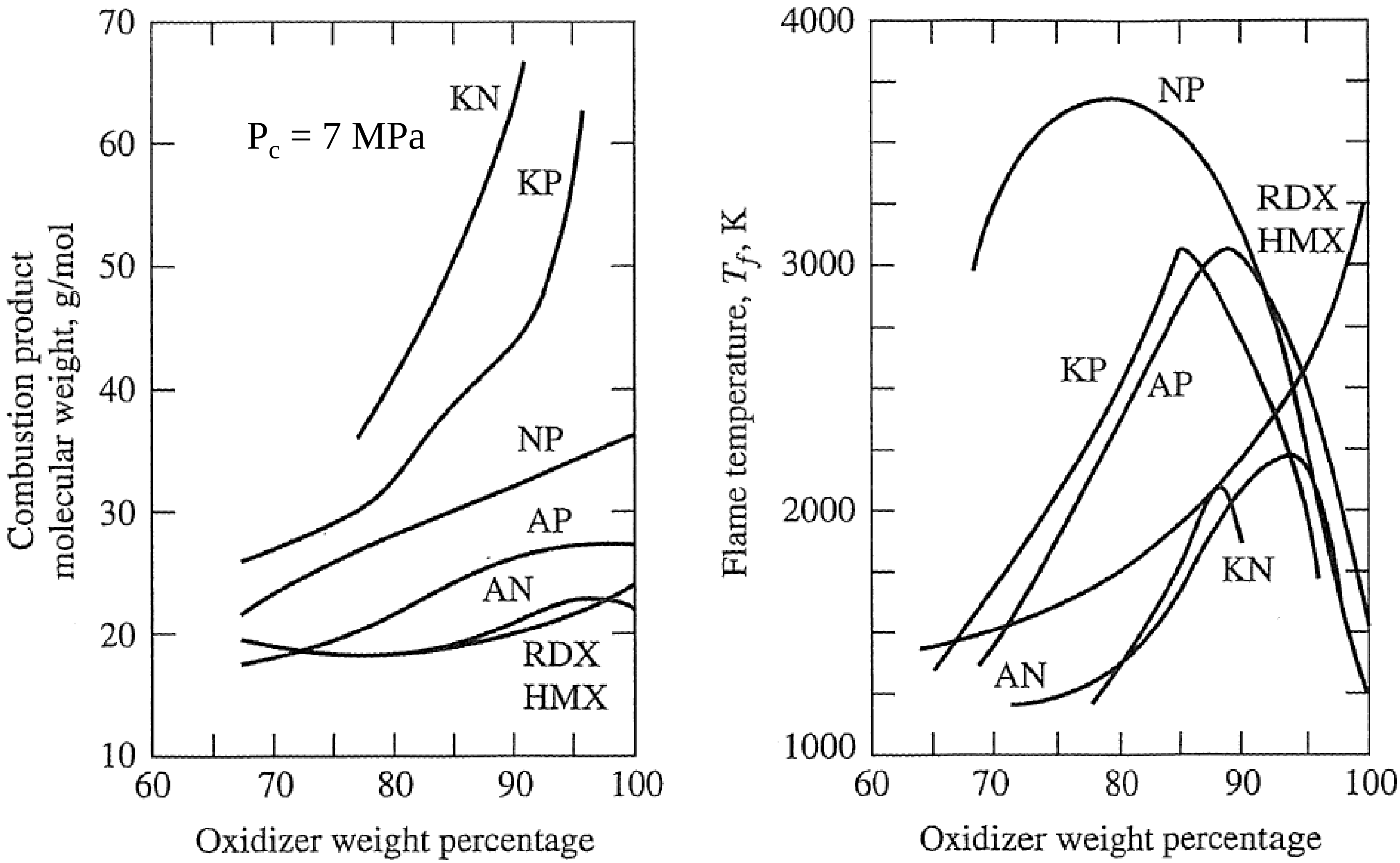

From Kuo and Acharya, 2012

Variation of I_{sp} of Several HTPB-based Solid Propellants with Oxidizer Concentration

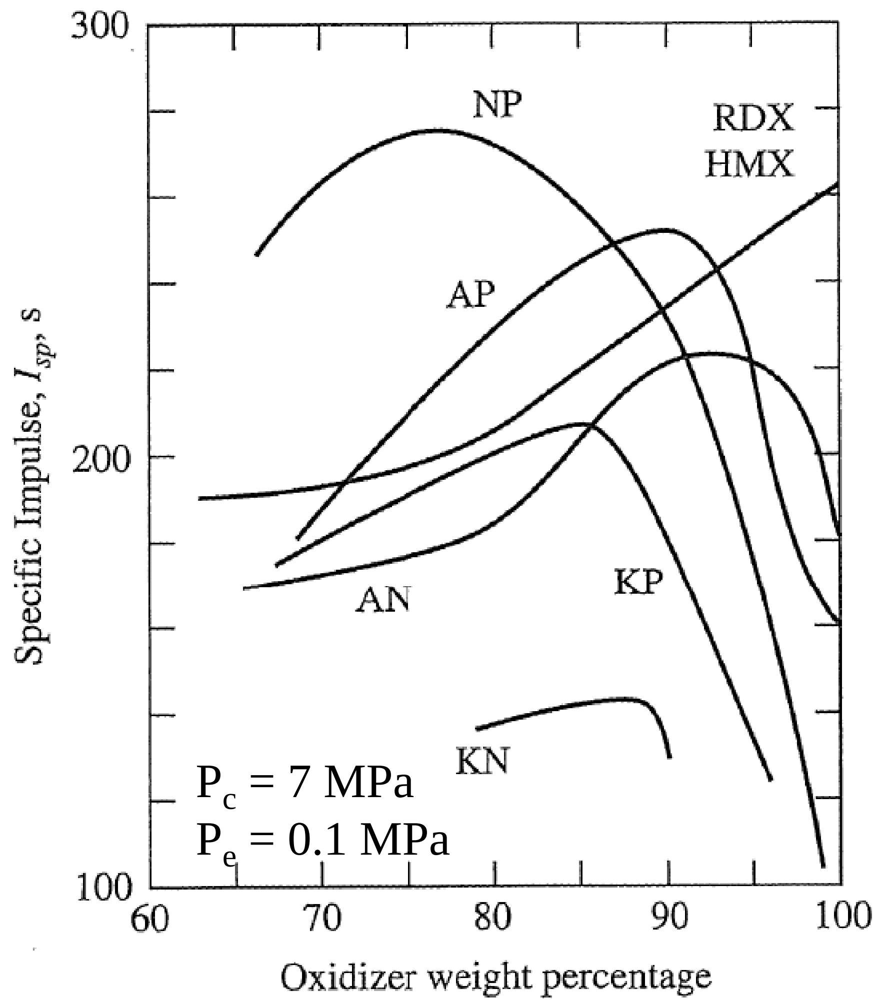

Nitronium perchorate (NP) shows the highest I_{sp}, but it is not a common oxidizer due to its low temperature decomposition initiating at 50°C.

From Kuo and Acharya, 2012